Conformational Changes in Cholera Toxin B Subunit−Ganglioside GM1 Complexes Are Elicited by Environmental pH and Evoke Changes in Membrane Structure†

Jameson A. McCann,‡ Jennifer A. Mertz,‡ John Czworkowski,§ and William D. Picking*,‡

Department of Biology, Saint Louis University, St. Louis, Missouri 63103-2010, and Department of Chemistry, Yale University, New Haven, Connecticut 06520

Received December 6, 1996; Revised Manuscript Received April 23, 1997⊗

ABSTRACT: Fluorescence resonance energy transfer (FRET) was used to monitor pH-dependent structural changes in the cholera toxin B subunit (CTB) and the membranes with which CTB associates. The distance separating the single tryptophan (Trp88) of each CTB monomer and a pyrene probe linked to the membrane-imbedded tail of ganglioside GM1 is not influenced by pH in a range from 3.5 to 7.5, consistent with the position of Trp88 in the GM1 binding site of CTB. In contrast, the distance between the pyrene probe on GM1 and coumarin, stilbene, or fluorescein probes covalently linked to specific sites on CTB appears to increase significantly as the pH is lowered to 5.0 or less. This conformational change is not accompanied by detectable changes in the distance between Trp88 and these extrinsic probe positions in the presence of nonfluorescent GM1. However, when the distance from Trp88 to the extrinsic probes is monitored as a function of pH in the absence of GM1, a conformational change is seen which indicates that receptor binding influences the character of pH-dependent conformational changes that occur within CTB. Interestingly, the observed change in CTB conformation is accompanied by a change in the relative position of GM1 within the membrane as judged by FRET from the pyrene probe on GM1 to a 7-nitrobenz-2-oxa-1,3-diazol-4-yl (NBD) probe linked to the polar head group of phosphatidylethanolamine and positioned at the membrane surface. Taken together, the data imply that low endosomal pH is capable of inducing structural changes in CTB, which, in turn, exert effects on the structure of the membrane to which CTB is bound. These phenomena may have a role in (1) processing of cholera toxin within the endosomal compartments of some target cell types, (2) determining the lag time between cholera toxin binding and the target cell response to cholera intoxication, or (3) the efficiency of CTB and cholera toxin as mucosal adjuvants.

The overt symptoms of cholera are well-known and the basic cellular events responsible for cytotoxicity of the *Vibrio cholerae* enterotoxin (CT)[1] have been thoroughly described (*1*−*3*). In contrast, molecular details of how the different subunits of the hexameric AB_5 complex of CT act together in initiating cellular intoxication remain poorly understood. CT (M_r = 85 620) binds cooperatively via its homopentameric B subunit (CTB) to ganglioside GM1 receptors on the apical surface of intestinal epithelial cells (*4*). This cooperativity is most likely related to the enhanced cooperative interactions known to occur between CTB monomers following the binding of GM1 (*5*) or the oligosaccharide moiety of GM1 (*6*). Upon binding, CTB forms a planar ring structure on the membrane surface which possesses a highly polar central pore that interacts intimately with the A2 polypeptide of CT. CTA2 is linked, in turn, to the A1 protein of CT by a disulfide bond (reviewed in *3*). Liberation of CTA1 by reduction of this disulfide linkage allows passage of CTA1 through the host membrane to sites where it ADP-ribosylates the GTP-binding regulatory protein $G_{s\alpha}$, leading to permanent activation of adenylate cyclase (*1*, *7*, *8*). These events result in the activation of sodium pumps via cAMP-dependent protein kinases and subsequent expulsion of sodium and water into the intestinal lumen (*9*). While CTB is clearly responsible for toxin binding to ganglioside GM1 receptors, an essential step in cholera intoxication, the mechanism for transport of CTA1 into the cytoplasmic compartment of target cells, remains unknown.

Determining the mechanisms responsible for CTA1 transport is important because, in addition to its well-known toxic effect, CT possesses potent mucosal adjuvant properties that can be exploited in oral immunization strategies (*10*, *11*).

† This work was supported by the Saint Louis University Beaumont Faculty Development Fund (Award 94-020) and Summer Research Award (Number 94-04) to W.D.P.; and by a 1995 American Society for Microbiology Undergraduate Research Award to J. A. Mertz.

* Corresponding author: Telephone (314) 977-3912; FAX (314) 977-3658; Email pickinwd@sluaxa.slu.edu.

‡ Saint Louis University.

§ Yale University.

⊗ Abstract published in *Advance ACS Abstracts,* July 1, 1997.

[1] Abbreviations: CT, cholera toxin; CTB, B subunit of cholera toxin; CTA1, A1 polypeptide of cholera toxin; CTA2, A2 subunit of CT; Trp88, single tryptophan residue of cholera toxin B subunit; GM1, monosialoganglioside GM1; pyrene-GM1, *N*-[12-(1-pyrenyl)dodecanoyl]-lyso-GM1; PC, phosphatidylcholine; NBD-PE, *N*-(7-nitrobenz-2-oxa-1,3-diazol-4-yl)-1,2-dipalmitoyl-L-α-phosphatidylethanolamine; fluorescein-DHPE, *N*-[(5-fluoresceinyl)thiocarbamoyl]-1,2-dihexadecanoyl-*sn*-glycero-3-phosphoethanolamine; CPI, 3-[4-(isothiocyanato)phenyl]-7-diethylamino-4-methylcoumarin; SITS, 4-acetamido-4′-(isothiocyanato)stilbene-2,2′-disulfonic acid; FITC, fluorescein isothiocyanate; Dns, dansyl chloride; FRET, fluorescence resonance energy transfer; CPI-CTB, cholera toxin B subunit covalently labeled with 3-[4-(isothiocyanato)phenyl]-7-diethylamino-4-methylcoumarin; Dns-CTB, cholera toxin B subunit covalently labeled with dansyl chloride; SITS-CTB, cholera toxin B subunit covalently labeled with 4-acetamido-4′-(isothiocyanato)stilbene-2,2′-disulfonic acid; FITC-CTB, cholera toxin B subunit covalently labeled with fluorescein isothiocyanate.

S0006-2960(96)02996-0 CCC: $14.00

Because many microorganisms invade their hosts via mucosal membrane surfaces, the development of a protective mucosal immune response can provide a preemptory line of defense against a variety of infectious diseases. Immunization against these pathogens by a parenteral route, while useful in eliciting a circulatory immune response, does little to generate effective protection against disease onset at mucosal surfaces due to the absence of an antibody response in mucosal secretions. Oral vaccines are able to induce production of secretory antibodies, but oral administration of purified antigens typically results in a weak immune response (*12*). An enhanced mucosal immune response to orally administered antigens can be achieved when the antigens are mixed with CT or conjugated to CTB (*13*−*15*). The ability of CT and CTB to act as mucosal adjuvants may stem from the adhesive and epithelial cell membrane-permeabilizing effects of these protein complexes (*11*, *16*); however, it appears that active toxin is more effective than the B subunit in exerting this immunostimulatory activity (*11*). It is therefore important to determine the events associated with CTB−membrane interaction and to identify mechanisms related to the potential translocational pathways of CTA1.

Studies of CT−membrane interactions have shown that CTB binding to GM1 incorporated into lipid bilayers induces the formation of membrane channels (*17*, *18*). These findings could indicate that CTA1 is translocated into the target cell cytoplasm by passing through a protein-lined pore that traverses the membrane. However, on the basis of investigations using membrane-imbedded photoactivatable probes (*19*) as well as low-resolution structural studies (*20*, *21*), it does not appear that CTB enters the membrane following its association with GM1 receptors. These studies could indicate that CT binds with CTA1 oriented toward the cell surface, thereby forcing CTA1 into and through the membrane upon CTB−GM1 interaction; however, such a mechanism is not consistent with the crystal structures of CT (*22*), CTB (*23*−*25*), and the closely related heat-labile enterotoxin of *Escherichia coli* (*26*, *27*). High-resolution structural analyses show that if the B pentamer of the toxin were bound with the A1 polypeptide oriented toward the membrane, a significant portion of the B subunit would also have to enter the membrane (reviewed in *3*). Moreover, recent evidence has demonstrated that functional CT binds with CTA1 facing away from the cell surface (*28*, *29*). These observations and the fact that CT does not appear to undergo significant structural changes upon receptor association (*3*) have prompted many questions concerning the mechanism by which CTA1 moves from a site that is some distance from the cell surface to take up a position within the target cell cytoplasm.

Evidence is now accumulating that supports a model in which endocytosis plays a major role in mediating cellular intoxication by CT (*30*−*35*). The role of endocytosis in mediating CT intoxication is not entirely clear; however, endosomal processing appears to involve CT migration to the Golgi and possibly other membrane-lined regions of the target cell cytoplasm (*30*, *34*, *35*). It now appears that endocytosis allows CT to encounter environmental stimuli that influence the course of cellular intoxication (*30*, *31*, *35*). The precise nature of these signals remains to be clearly established, but it is reasonable to suggest that one environmental condition encountered by CT following endocytic uptake is lowered pH. In fact, low pH has been suggested to be important in CT intoxication of rat hepatocytes (*30*, *31*) and may influence the membrane-permeabilizing effects of CTB (*17*, *36*). Moreover, low pH has been suggested to have a role in cellular intoxication by other AB_5 toxins (*37*, *38*).

To investigate the effects of low pH on the structural properties of CTB and associated membranes, fluorescence resonance energy transfer (FRET) was used to monitor pH-dependent changes in the distance between various sites on CTB and phospholipid vesicles containing GM1. Previous findings have shown that the structure of GM1-containing membranes is altered by CTB binding and that pH may influence this effect (*36*). These results and the findings presented here demonstrate that endosomal pH evokes conformational changes in CTB which, in turn, influence the properties of associated GM1-containing membranes. Whether these events participate directly in CTA1 translocation is not yet clear; however, these observations provide insight into structural events that could occur following endocytic uptake. The data presented here take on increased significance in light of recent findings that CT may move by transcytosis from the apical to the basolateral membrane of intestinal epithelial cells, where the ultimate protein target of CTA1 is located (*33*). Such a scenario would appear to increase the likelihood that CT spends a considerable amount of time within an acidified endosomal compartment. It will now be important to extend these studies to take into account the position of CTA1 relative to the membrane under endosomal conditions.

MATERIALS AND METHODS

Materials

CTB was purchased from List Biological Laboratories, Inc. (Campbell, CA). Ganglioside GM1, pyrene-GM1, bovine liver phosphatidylcholine (PC), dimethylformamide (DMF), dansyl chloride (Dns), and fluorescein isothiocyanate (FITC) were purchased from Sigma Chemical Co. (St. Louis, MO). 3-[4′-(isothiocyanato)phenyl]-7-diethylamino-4-methylcoumarin (CPI), 4-acetamido-4′-(isothiocyanato)stilbene-2,2′-disulfonic acid (SITS), *N*-(7-nitrobenz-2-oxa-1,3-diazol-4-yl)-1,2-dipalmitoyl-L-α-phosphatidylethanolamine (NBD-PE), and *N*-[(5-fluoresceinyl)thiocarbamoyl]-1,2-dihexadecanoyl-*sn*-glycero-3-phosphoethanolamine (fluorescein-DHPE) were from Molecular Probes, Inc. (Eugene, OR). Methanol was from Fisher Scientific (St. Louis, MO). All other chemicals were of reagent grade.

Methods

Preparation of PC Vesicles. Phospholipid vesicles were prepared by drying 1 mg of PC (in 3:1 chloroform:methanol) under a stream of nitrogen followed by further removal of solvent in a vacuum for 1 h at 37 °C. The PC was dispersed in 1 mL of buffer (50 mM sodium citrate−50 mM sodium phosphate, pH 7.0, and 0.15 M NaCl) by sonication at room temperature with three 30-s bursts (Fisher Scientific 550 Sonic Dismembrator, microtip, 20 kHz). Vesicles were allowed to form by incubating the sample at 37 °C followed by incubation overnight at room temperature to allow formation of large unilamellar vesicles. All vesicle preparations were used within 4 days.

To incorporate GM1, pyrene-GM1, NBD-PE, or fluorescein-DHPE into the outer leaflet of PC vesicles, each was added

Table 1: Fluorescence Quenching of Labeled Lipids Present on the Outer Leaflet vs the Inner and Outer Leaflets of PC Vesicles

	K_Q[b] (M^{-1}) for NBD-PE located on	
quenching agent[a]	inner and outer leaflets[c]	outer leaflet only[d]
acrylamide	0.209	0.439
iodide	0.777	1.742
methylviologen	1.768	5.054

[a] All three quenching agents are polar and should not cross phospholipid membranes. Acrylamide is a neutral quenching agent, iodide is anionic, and methylviologen is a divalent cation. [b] The Stern−Volmer quenching constant (K_Q) was determined according to the relationship described originally by Stern and Volmer (*40*). [c] To place fluorescent lipids on both the inner **and** outer leaflets of PC vesicles, they were included in the dried PC mixture that was sonicated in buffer containing 0.15 M NaCl. [d] To incorporate fluorescent lipids into the outer leaflet of PC vesicles, they were added from a methanol stock to preformed vesicles in buffer containing 0.15 M NaCl.

(from a stock solution in methanol) to preformed PC vesicles and the sample was incubated at least 1 h at 37 °C. That incorporation of fluorescent lipids into the membranes had occurred could be observed with pyrene-GM1 by monitoring conversion of pyrene fluorescence from an excimer to a monomer state (*39*). To confirm that incorporation of fluorescent lipids was essentially limited to the outer leaflet of the preformed vesicles, fluorescence quenching was used to monitor the accessibility of polar quenching agents to the probe. Quenching of fluorescence from probes present only on the outer leaflet was compared to quenching of labeled lipids that were sonicated with PC to place them on both the inner and outer leaflets of the membrane (Table 1). The presence of a fluorescent probe population on the inner leaflet would result in decreased accessibility to polar quenching agents relative to vesicles with probes limited to the outer leaflet.

When excited fluorophores collide with small quenching agents like acrylamide, methylviologen (1,1′-dimethyl-4,4′-bipyridinium), or iodide, they return to their ground-state without photon emission. Such quenching processes were quantified by Stern and Volmer (*40*), who developed the following relationship:

$$F_0/F = 1 + K_Q[Q] \quad (1)$$

where F_0 is the probe's fluorescence intensity in the absence of quenching agent, F is the fluorescence intensity at a given concentration of quenching agent (given by [Q]), and K_Q is the Stern−Volmer quenching constant. K_Q is given by the slope of a plot of F_0/F vs [Q] and provides a measure of probe accessibility to quenching agents. Fluorescent lipids present only on the outer leaflet of PC vesicles should be quenched more efficiently than those on the inner leaflet due to greater accessibility to the external aqueous environment. Therefore, larger apparent K_Q values should be seen for vesicles with fluorescent lipids limited to their outer leaflet than for vesicles with fluorescent lipids present on both leaflets. For each quenching agent tested, the quenching of NBD-PE was substantially greater when the probe was incorporated into the outer leaflet of the vesicle rather than both the outer and inner leaflets (Table 1), indicating that fluorescent lipid incorporation was essentially limited to the exposed surface of the PC vesicles.

Fluorescence Labeling of CTB. To label CTB at primary amines, the protein was first passed over Sephadex G25 equilibrated with 0.1 M carbonate (pH 8.5). The sample could be labeled directly with 5 mM FITC or SITS, or it could be made 50% DMF for labeling with 2 mM CPI or Dns. The sample was incubated 30 min at 37 °C and any precipitate that formed was removed by centrifugation. Labeled CTB was separated from unreacted dye and solvent by gel filtration on Sephadex G50 equilibrated with 50 mM phosphate (pH 7.5), 0.15 M NaCl, and 1 mM sodium azide. Fluorescent fractions were collected and the CTB and probe concentrations determined by absorbance at 280 nm and the peak of dye absorbance, respectively. SDS−polyacrylamide gel electrophoresis (*41*) was used with UV detection to ensure that samples contained labeled protein that was free of contaminating unreacted dye.

In most cases, CTB was labeled to a stoichiometry near 1 probe/monomer. FITC slightly exceeded this labeling stoichiometry (1.1 probes/CTB monomer), while the more nonpolar probes labeled to a slightly lower stoichiometry (0.75 for CPI). A greater labeling ratio could be obtained with CPI by completely denaturing CTB with 6 M guanidine hydrochloride, but this approach led to much greater diversity in the sites to which CPI was attached. Mass spectrometric analyses revealed that the majority (>80%) of the CTB was monolabeled with FITC, with a small amount of dilabeled CTB present. Proteolytic digestion of CTB with V8 protease, followed by peptide separation and amino acid sequence analysis, was performed to determine the specific CTB site-(s) labeled with fluorescent probe. These analyses revealed that nearly all of the labeled CTB was modified at either Lys69 or Lys91. CPI labeling, carried out in the presence of 50% DMF, resulted in greater diversity in the specific sites modified but with Lys69 and Lys91 appearing to be the primary labeling sites. In all cases, the FRET results obtained using CPI-CTB or Dns-CTB were the same as those using FITC- or SITS-labeled CTB.

For binding CTB (labeled or unlabeled) with GM1-containing vesicles, the vesicles (with GM1 or pyrene-GM1 already incorporated) were incubated with CTB for 15−30 min at 37 °C. It was possible to monitor the extent of binding by monitoring the extent of the blue shift in the emission spectrum of Trp88 (*36*).

Fluorescence Measurements. Steady-state fluorescence spectroscopy was carried out on a Spex (Edison, NJ) FluoroMax spectrofluorometer with temperature-controlled sample compartment, automatic blank subtraction, correction for wavelength dependence of lamp intensity, and removable excitation and emission polarizer assemblies (for polarization and anisotropy measurements). Wavelengths for fluorescence excitation were 282 nm for Trp88, 330 nm for pyrene, 385 nm for CPI, and 480 nm for FITC. Fluorescence data were collected at the emission maximum for each probe at a scanning rate of 0.1 s/wavelength increment and with a sample absorbance of less than 0.1 at both the excitation and emission wavelengths to avoid an inner filter effect.

Distance Determination Using Fluorescence Resonance Energy Transfer. FRET is the passage of excitation energy from a donor fluorophore (d) to an acceptor (a) molecule whose absorption spectrum overlaps the donor emission spectrum. FRET efficiency for a d−a pair is dependent upon three main factors: (1) the degree of overlap between d emission and a absorption (given by the spectral overlap integral J), (2) the relative orientation of d and a dipoles (described by κ^2 and ranging from 0 to 4), and (3) the distance separating d and a. If the J and κ^2 values are known

Table 2: Fluorescence Resonance Energy Transfer Parameters

		Φ^a		R_0 (Å)	
donor	acceptor	pH 7.5	pH 3.5	pH 7.5	pH 3.5
Trp88	pyrene-GM1	0.28	0.22	30.1	29.1
pyrene-GM1	CPI-CTB	0.05	0.05	27.6	27.6
pyrene-GM1	SITS-CTB	0.05	0.05	25.5	25.5
pyrene-GM1	FITC-CTB[b]	0.05	0.05	23.1	15.5
Trp88	CPI-CTB (−GM1)	0.26	0.04	32.1	24.4
Trp88	CPI-CTB (+GM1)	0.28	0.22	33.3	30.8

[a] The fluorescence quantum yield of the donor was calculated on the basis of comparisons with a quinine sulfate standard (*48*). [b] While the quantum yield of pyrene-GM1 did not change as a consequence of low pH, a large decrease in the absorption of FITC-CTB resulted in the dependence of R_0 on environmental pH for this donor−acceptor pair.

for a d−a pair, FRET efficiency (E) becomes useful for calculating inter- and intramolecular distances (*42*). More importantly, E provides an extremely sensitive measure of structural changes within a macromolecular complex. Therefore, E was used to monitor distances between different sites within CTB and GM1-containing membranes as a function of environmental pH.

For a given d−a pair, J is readily calculated using spectral measurements, while the relative orientation of donor and acceptor dipoles is more difficult to assess. In situations involving probes attached to proteins or membrane components, the relative dipole orientation is typically considered random ($\kappa^2 = {}^2/_3$), which assumes that each dipole adopts a dynamically averaged orientation over the fluorescence lifetime of d. Unfortunately, assuming a random orientation factor can introduce significant error into the resulting distance determinations if κ^2 deviates far from a dynamically averaged value (*43*). Estimation of the uncertainty introduced by not knowing κ^2 is possible by a variety of approaches (*43*, *44*). Also, a convincing argument is presented by dos Remedios and Moens (*45*) for confidently using FRET to measure protein conformational changes even without knowledge of κ^2. They present a strong case in which intraprotein distances determined from crystallographic studies is in general agreement with those determined in FRET studies using $\kappa^2 = {}^2/_3$ when the size of the probes are taken into consideration (*45*). More importantly, however, with or without knowledge of κ^2, FRET provides one of the most convenient and sensitive tools for detecting conformational changes in macromolecular complexes. For the distance determinations here, half-height limits were estimated by establishing the extent of isotropical randomization of d and a on the basis of their fluorescence anisotropy and polarization values (*43*). Anisotropy values were determined essentially as described by Odom et al. (*46*).

FRET efficiency (E) can be calculated from

$$E = 1 - (F_{da}/F_d) \tag{2}$$

where F_{da} is the fluorescent intensity of d in the presence of a and F_d is the fluorescence intensity of d in the absence of a. To calculate the distance separating a given d−a pair, it was first necessary to determine the Förster distance (R_0) which describes the distance giving 50% E (see Table 2) (*47*) according to the following relationship:

$$R_0 \text{ (in Å)} = (9.79 \times 10^3)(\kappa^2 n^{-4} \Phi_d J)^{1/6} \tag{3}$$

where n is the refractive index of the medium separating d and a and Φ_d is the fluorescence quantum yield of d. The latter was determined by comparison with a quinine sulfate standard in 0.1 N H_2SO_4 (*48*). In some experiments, the dependence of donor quantum yield or acceptor absorbance on pH made it necessary to determine R_0 for each pH tested (see Table 2). Once E and R_0 were known, they were used to calculate the distance separating the donor and acceptor according to the following relationship:

$$E = R_0^6/(R_0^6 + r^6) \tag{4}$$

where r is the calculated distance between d and a.

A factor that complicates these distance determinations is the possibility that multiple donors can be paired with multiple acceptors within the pentameric CTB−GM1 complexes. When the distance between multiple acceptors and donors is asymmetric, the inverse sixth power relationship between E and r ensures that the acceptor nearest each donor dominates the energy transfer process. In contrast, multiple equidistant acceptors requires a modified analysis of FRET as detailed by Highsmith and Murphy (*49*). It is known in this case that the arrangement of donors relative to acceptors is asymmetric given the distances from Trp88 to the α-carbons of Lys69 and Lys91 in the published crystal structure of CTB (*22*−*24*). This asymmetry is assumed to hold for fluorophores linked to the ϵ-amino group of these lysine residues. It is also assumed that acceptor probes at Lys69 and Lys91 are asymmetrically positioned relative to the pyrene label on GM1, which appears to be approximately centered below Trp88 at the membrane surface. It is possible that these assumptions introduce a modest error into the determined distances; however, this does not lessen the significance of the conformational changes detected within the CTB−GM1 complex.

FRET Measurements. To determine E from Trp88 to pyrene-GM1, the fluorescence intensity of Trp88 was measured at the peak of Trp88 emission (338 nm) with F_d measured using nonfluorescent GM1 and F_{da} measured using pyrene-GM1. The lack of a red shift in the Trp88 emission spectrum provided evidence that CTB remained associated with its ganglioside receptor at each pH tested (*50*). To determine E for energy transfer between membrane-imbedded pyrene-GM1 and a CPI or SITS acceptor covalently linked to CTB (see above), pyrene fluorescence intensity was measured at its second emission peak (398 nm). F_d was measured with pyrene-GM1 bound to unlabeled CTB, and F_{da} was measured with pyrene-GM1 bound to fluorescent CTB. For FRET from Trp88 to an extrinsic fluorophore linked to CTB (CPI, Dns, or SITS), E was calculated both in the presence and in the absence of nonfluorescent GM1. In this case, Trp88 emission was measured at its peak of fluorescence (350 nm in the absence of GM1 or 338 nm in the presence of GM1) with F_d measured using unlabeled CTB and F_{da} measured using the same concentration of labeled CTB.

To determine the distance from probes attached to the hydrophobic tail of pyrene-GM1 or sites on CTB, to acceptors present at the surface of PC vesicles, either NBD-PE (an acceptor for CPI, SITS, pyrene, or Trp88) or fluorescein-DHPE (an acceptor for CPI or SITS) was preincubated with PC vesicles prior to incorporation of GM1 and the binding of CTB. Initial experiments were designed to determine the amount of fluorescent phospholipid needed to obtain approximately 50% E and that amount (see figure

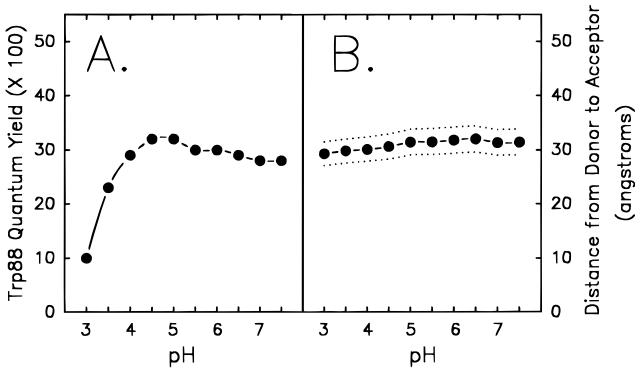

FIGURE 1: Distance from Trp88 to pyrene attached to the nonpolar tail of GM1 does not vary with pH. In panel A, low pH influences the Trp88 quantum yield which is needed for calculation of R_0 (see Table 2). Quantum yield was determined as described under Methods using an excitation wavelength of 282 nm. In panel B, energy transfer was used to calculate the distance between Trp88 (150 nM CTB) and the pyrene label on GM1 (5 μM), incorporated into 0.1 mg/mL PC vesicles, as a function of pH (solid line with symbols). The dotted lines show the upper and lower half-height limits of uncertainty in the distance determinations based upon a Trp88 polarization value of 0.30 and a pyrene-GM1 polarization value of 0.15.

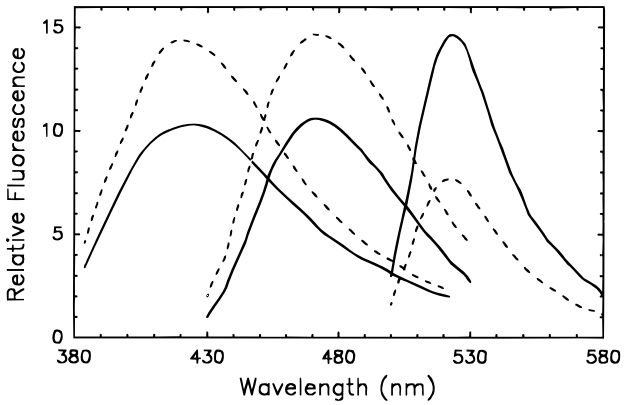

FIGURE 2: Effect of GM1 binding on the fluorescence emission spectra of 0.3 μM SITS-CTB (left; excitation at 330 nm and emission maximum at 420 nm), 0.1 μM CPI-CTB (center; excitation at 385 nm and emission maximum at 472 nm), and 0.1 μM FITC-CTB (right; excitation at 490 nm and emission maximum at 523 nm). In each case, the solid line shows the emission spectrum of labeled CTB in the absence of GM1 and the dashed line shows the relative emission spectrum of the same concentration of labeled protein in the presence of at least a 5-fold molar excess of GM1 mixed with PC vesicles.

legends) was then used in subsequent experiments where pH served as the only variable. As above, E was determined from emission spectra spanning the expected fluorescence of the donor and acceptor probes. The effect of pH on the absorption of the acceptor probe was determined before conclusions were made concerning changes in the position of probes on GM1 and CTB relative to the surface of the PC vesicles. Also, no specific distance calculations were performed using these FRET determinations because the observed FRET is merely an average value that is dependent upon acceptor density on the surface of the phospholipid vesicles.

RESULTS

Distance from Trp88 to Pyrene-GM1 Is Not Influenced by pH. FRET data were used to calculate the distance from Trp88 of CTB to a membrane-imbedded pyrene acceptor linked to the hydrophobic tail of GM1 and the effects of pH on this distance were then monitored. Because (1) R_0 is a function of donor quantum yield (Φ) and (2) quantum yield can be influenced directly by pH (Figure 1A), it is necessary to calculate R_0 for the Trp88 donor at each pH examined (Table 2). When these changes in the Trp88 quantum yield are considered, no change in the calculated distance between the two sites is seen (Figure 1B). Moreover, the apparent distance separating the pyrene and Trp88, about 32 Å, is in general agreement with the anticipated distance between these sites based on the fact that Trp88 is located within the GM1 binding site of CTB (*23*, *24*). It is not necessarily surprising that this calculated distance remains constant as a function of pH since a change in distance would require reorientation of the nonpolar acyl moiety of GM1 within the lipid bilayer or a major distortion of the GM1 binding site of CTB. Therefore, to determine if pH has an effect on the structure of CTB following its association with GM1, it is necessary to label this protein with an extrinsic fluorescent probe at sites other than Trp88.

Distance from the Membrane-Imbedded Pyrene to Extrinsic Probes Covalently Linked to CTB Is Influenced by pH. CTB was modified with extrinsic fluorescent labels to provide probes at sites distinct from Trp88. CTB was labeled at accessible primary amines (lysines) with CPI, SITS, or FITC, each of which labels to a stoichiometry that approached 1 probe/CTB monomer (data not shown). Because there are up to nine potential labeling sites on CTB (*51*, *52*), these results suggest that only one or a limited number of residues are readily available for covalent modification with amine-reactive fluorescent probes under the labeling conditions used. To provide quantitative significance for FRET measurements from pyrene-GM1 to the extrinsic probes on CTB, it was necessary to determine the position of these labeled sites for at least one of the extrinsic probes. Accordingly, FITC-CTB and CPI-CTB were digested with V8 protease at glutamate residues and the peptide fragments were resolved by reversed-phase high-performance liquid chromatography (RP-HPLC) for mapping of labeling sites.

From mass spectrometry and peptide sequence analysis, it was determined that the majority (>80%) of the CTB monomers labeled with FITC are present as monolabeled species with relatively small populations of unlabeled and dilabeled species (data not shown). Following proteolytic digestion and sequence analysis, only two residues appeared to be significantly involved in the labeling process, Lys91 and Lys69. Lys91 is present at the edge of the GM1 binding site of CTB (about 10 Å from Trp88 on the same CTB monomer) and may be involved in interactions with the terminal galactose moiety of GM1 (*23*, *24*). Lys69 is located at the middle of the large central helix of CTB (*26*) but is relatively near the GM1 binding region (about 17 Å from Trp88 on the same CTB monomer) according to the published CTB crystal structure (*22*−*24*). The ability of labeled CTB pentamers to actively bind pyrene-GM1 is demonstrated by observed FRET from pyrene to CPI-CTB, SITS-CTB, or FITC-CTB (see below). Moreover, that labeled CTB monomers (within active CTB pentamers) participate in GM1 binding is suggested by changes in the fluorescence of the extrinsic probes upon incubation with unlabeled GM1 (Figure 2). In fact, by monitoring changes in fluorescence as a function of GM1 concentration, we have

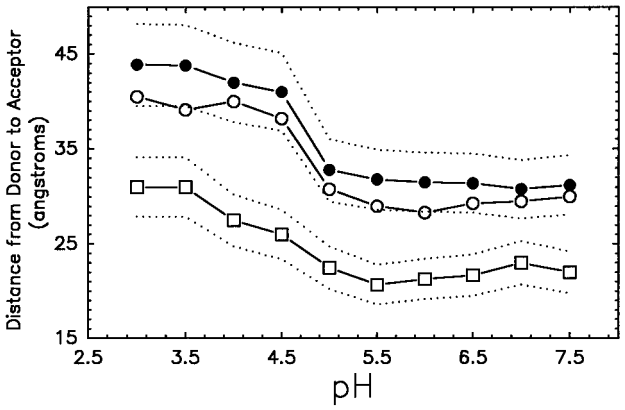

FIGURE 3: Distance from pyrene attached to the hydrophobic tail of GM1 to CPI, SITS, or FITC covalently linked to CTB (at Lys69 or Lys91) increases at low pH. Pyrene-GM1 (150 nM) was incorporated into PC vesicles (0.1 mg/mL) and excited at 330 nm. Its apparent distance from the extrinsic probe on CTB was then determined by FRET using 300 nM CPI-CTB (●), SITS-CTB (○), or FITC-CTB (□). Energy transfer was calculated from quenching of pyrene-GM1 fluorescence at its 400 nm peak of fluorescence. The dotted lines show the upper and lower half-height limits of uncertainty in the distance calculations for experiments involving CPI-CTB (upper set) and FITC-CTB acceptors (lower set). These uncertainty values are based upon a pyrene-GM1 polarization of 0.15, a CPI-CTB polarization of 0.30, and an FITC-CTB polarization of 0.20. The R_0 for the pyrene-GM1/CPI-CTB and pyrene-GM1/SITS-CTB donor/acceptor pairs remained essentially constant throughout these experiments because pH had no effect on the quantum yield of the pyrene sequestered at the interior of PC vesicle membranes or the absorption of the CPI or SITS. R_0 did change as a function of pH when FITC-CTB was used as the acceptor due to the reduction of FITC absorption at low pH (see Table 2).

observed that the dissociation constant of labeled CTB for GM1 appears to remain within an order of magnitude of that seen for unmodified CTB (data not shown).

As demonstrated in Figure 3, when CPI-CTB or SITS-CTB is bound to pyrene-GM1 incorporated into PC vesicles, the apparent distance from the membrane-imbedded pyrene to the extrinsic probe on CTB increases by 10 Å or more as the pH is reduced to about 4.5 or less. This apparent change in distance occurs without an accompanying change in the quantum yield of the pyrene and with no significant change in the absorption spectrum of the coumarin or stilbene acceptor probes in the pH range tested. The absence of an emission spectrum change for the membrane-imbedded pyrene-GM1 (data not shown) suggests that the observed results do not reflect an artifact of pyrene-GM1 extraction from the membrane. Similar results are seen when FRET is carried out from pyrene-GM1 to a FITC probe linked to CTB (Figure 3). In the latter experiment, a much smaller change in the apparent distance (about 5 Å) from pyrene to the labeled site on CTB is observed; however, a relatively sharp transition in the distance separating the probes is still apparent between pH 5.5 and 4.5 (Figure 3).

Interestingly, at each pH, the distance from the pyrene to FITC is always less than the distance to CPI or SITS. This can be explained, at least in part, by the minor differences in the labeling stoichiometry of these probes, which possess different chemical characteristics. As already mentioned, FITC labeling occurs with a stoichiometry just greater than 1, while CPI labels with a stoichiometry slightly less than 1. SITS labeling also occurs with a stoichiometry that is slightly less than 1. Another possible contributing factor to the difference in distances determined using FITC and CPI

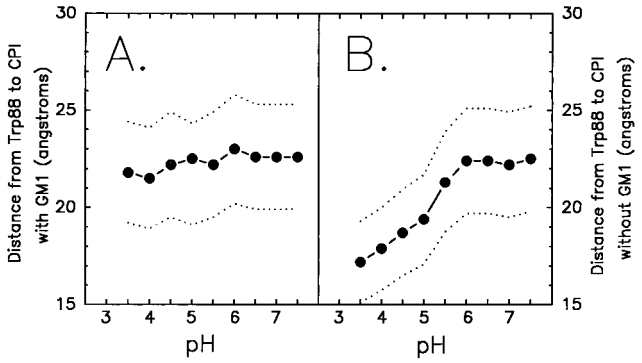

FIGURE 4: Distance from Trp88 to an extrinsic probe attached to CTB is not affected by low pH in the presence of GM1. Trp88 was excited at 282 nm and energy transfer was used to determine its apparent distance from CPI in the presence (A) or absence (B) of ganglioside GM1. F_d was measured with 300 nM unlabeled CTB and F_{da} was measured with the same concentration of CTB that had been labeled with CPI. The dotted lines show the upper and lower half-height limits of uncertainty in the distance determinations based upon a Trp88 polarization value of 0.30 and a CPI-CTB polarization value of 0.3.

(or SITS) could be the probes being oriented differently on the protein due to their relative polarities/hydrophobicities. Such differences in orientation would be accommodated by the long, flexible side chain of lysine. In any case, the data using each probe lead to the same conclusion that low pH induces a change in CTB conformation (and/or the structure of the membrane to which it attaches), which causes a significant increase in the distance between the pyrene label on GM1 and the sites on CTB occupied by extrinsic fluorescent probes.

Distance from Trp88 to a Coumarin Probe Attached to CTB Is Not Influenced by pH in the Presence of GM1. To investigate whether the distance change described above is seen using Trp88 as the donor probe, FRET was used to measure the distance from Trp88 to the extrinsic probe presumably linked to the same CTB monomer (but possibly present on an adjacent monomer). As shown in Figure 4A, pH has little effect on the distance separating Trp88 and CPI in the presence of nonfluorescent GM1. Identical results are obtained when a dansyl (Dns) probe is used to label CTB (data not shown). In the absence of GM1, low pH results in a decrease in the distance between Trp88 and the CPI probes (Figure 4B). Interestingly, the distance from Trp88 to the probes at Lys69 and Lys91 appears to be greater than the distance that would be anticipated on the basis of the crystal structure of CTB (*22*−*24*). Moreover, the presence of acceptor probes on adjacent CTB monomers that are also within the R_0 distance for the Trp88/CPI pair suggests that additional contributions to the Trp88 transfer decay should further reduce the apparent distance between probes. This discrepancy is due, in part, to a labeling stoichiometry of less than 1 for CPI and Dns; however, an unfavorable orientation of the probes may also have a role in the calculated distance between Trp88 and CPI. Another possibility is that the long and flexible side chain of lysine (or the phenyl group linker on CPI) causes the acceptor probe to be more distant from Trp88 than would be predicted from the CTB crystal structure.

Despite possible discrepancies in the calculated distances, the data presented in Figure 4 support previous findings in this laboratory and the observations by others that GM1 binding stabilizes the structure of CTB against denaturation

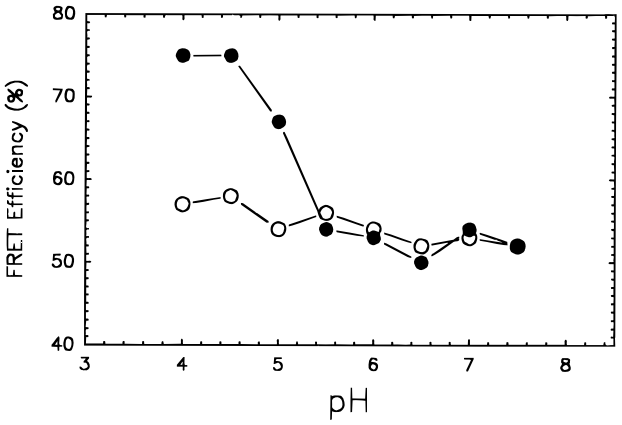

FIGURE 5: CTB elicits changes in the position of the hydrophobic tail of GM1 relative to the surface of the membrane as a function of pH. NBD-PE (at a final concentration of 4 μg/mL) was incorporated into the outer face of PC vesicles (0.1 mg/mL) along with 160 nM pyrene-GM1. FRET was then measured from the pyrene (excitation at 330 nm and emission measured at the 398 nm peak of pyrene fluorescence) to surface NBD linked to the polar head group of phosphatidyl ethanolamine. FRET was determined from pH 4.0 to 7.5 in the absence (○) or presence (●) of CTB.

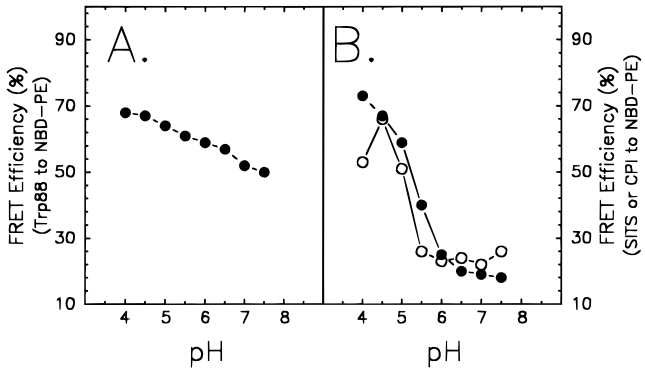

FIGURE 6: Movement of fluorescent probes on CTB relative to the surface of GM1-containing vesicles as a function of pH. In panel A, Trp88 fluorescence (0.33 μM CTB) was excited at 282 nm and energy transfer to NBD-PE (4 μg/mL) was measured as a function of pH. In panel B, FRET from SITS (○) or CPI (●) on CTB to NBD (4 μg/mL NBD-PE) at the surface of PC vesicles was determined as a function of pH. All of these experiments were performed at least three times and provided similar results.

and collapse at low pH (*5*, *6*, *53*, *54*). However, when all the data are considered, it appears that a structural change in the CTB−GM1 complex is elicited by low pH. Because there is no change in the distance from Trp88 to extrinsic probes on CTB in the presence of GM1, a relatively minor conformational change in CTB may elicit a disturbance in membrane packing, perhaps via a change in the relative orientations of the pentamer subunits, that causes the distance from the nonpolar tail of pyrene-GM1 to extrinsic probes on CTB to increase substantially. The latter would have to occur without a change in the distance from Trp88 to the tail of pyrene-GM1.

Low pH Effects on CTB Conformation Correlate with Changes in the Position of Pyrene-GM1 within the Phospholipid Membrane. Previous data from this laboratory suggest that CTB binds to pyrene-GM1 incorporated into PC vesicles to cause localized disruption of membrane structure (*36*). This disturbance in phospholipid packing is diminished when the pH is lowered to about 5.0 or less (*36*). These data may indicate that endocytic pH is able to promote conformational changes in CTB that influence membrane structure. According to the data presented in Figure 3, it is unlikely that this phenomenon is due to extraction of the fluorescent GM1 from the membrane. To investigate whether movement of GM1 relative to the rest of the membrane contributes to the observed change in distance from the pyrene on GM1 and the extrinsic probes on CTB, FRET was used to monitor the position of the pyrene group with respect to the surface of the PC vesicle. NBD-PE was incorporated into the outer face of vesicles and FRET was used to look for changes in distance between membrane-imbedded pyrene and surface-associated NBD in the presence and absence of CTB. In the absence of CTB, pH has almost no effect on FRET between the pyrene and NBD probes (Figure 5); however, FRET increases substantially beginning at pH 5.0 in the presence of excess CTB (Figure 5). These data provide convincing evidence that CTB binding to GM1-containing membranes mediates pH-dependent changes in membrane structure. Moreover, the net movement of the imbedded pyrene probe on GM1 appears to be toward the surface of the membrane but does not involve extraction of the acyl tail of GM1 from the nonpolar membrane interior. In other words, low pH induces changes in the membrane-bound CTB that allow it to pull GM1 toward the membrane surface.

Effect of Low pH on the Position of Extrinsic Probes on CTB Relative to the Membrane Surface. To look for changes in the distance between Trp88 and the membrane surface as a function of pH, NBD-PE was incorporated into PC vesicles to serve as a FRET acceptor while Trp88 served as a fluorescence donor. In these experiments, FRET from Trp88 to the membrane surface was found to increase as the pH was lowered (Figure 6A); however, the observed change in FRET occurred gradually and over a rather broad pH range. The gradual nature of these changes in FRET suggests that the lowering of pH causes subtle changes in the spectral characteristics of one or both of the probes used in these measurements rather than an abrupt pH-dependent conformational change in the CTB/GM1 complex.

In contrast, when a similar experiment is carried out to monitor FRET from extrinsic probe sites on CTB (CPI or SITS) to NBD at the surface of the GM1-containing vesicles, a rapid and significant increase in FRET is observed at a pH of 5.0 or below (Figure 6B). These data imply that pH conditions that result in movement of the extrinsic probes on CTB away from the pyrene on GM1 and movement of the same pyrene toward the membrane surface also result in the apparent movement of extrinsic probes on CTB toward the membrane surface. The last motion is reflected in a significant increase in the FRET efficiency from the pyrene on GM1 to NBD probes at the membrane surface.

DISCUSSION

Although the major steps in cholera intoxication have been described (*1*, *2*), molecular details on the CT and membrane structural properties that accompany cellular intoxication and ultimately result in CTA1 entry into the target cell cytoplasm remain obscure. Recent lines of evidence from a number of laboratories implicate endosomal processing as an important aspect of CT intoxication (*31*−*35*). Moreover, Lencer et al. (*33*) suggest that transcytosis of CT from the apical face to the basal region of enterocytes probably is an important step in CT processing. In such a scenario, it is

possible that CT spends a significant amount of time in a moderately low pH environment. Indeed, endosomal pH has been suggested to play an important role in CT intoxication of rat hepatocytes (*30*, *31*) and endosomal processing and low pH may contribute to intoxication of cells by some other AB_5 subunit toxins (*37*, *38*); however, this may not hold true for CT in all model systems (*35*). In fact, if trafficking of CT to the Golgi or trans-Golgi region is important for CT intoxication of epithelial cells, the toxin may spend most of its time at a pH nearer to 5.5, which is only at the threshold of the pH needed to induce the CTB conformational changes described here. It is important, however, to note that CT and CTB, as adjuvants, may take a number of relevant pathways in antigen presentation at mucosal surfaces, and some of these pathways could easily involve endosomal processing in acidic environments.

CTB has been shown to consist of two folding domains with each having a different stability to low pH and strong denaturants (*55*). It has been suggested that interactions between these domains (within and between CTB monomers) is responsible for the cooperative folding of the CTB pentamer (*55*). It is likely that these pH-sensitive interactions also participate in the cooperative interactions that occur between CTB monomers upon binding GM1 (*5*) or the oligosaccharide of GM1 (*6*). The net result of these interactions is a GM1-induced stabilization of the CTB pentamer structure (*5*, *6*, *53*, *54*), which could also account for cooperative binding of GM1 (*4*). To date, however, there have been relatively few detailed studies on the influence of endosomal pH on the known structural features of the CT/GM1 complex *and* how these features, in turn, influence the structure of GM1-containing membranes.

Fluorescence analyses were used to investigate the structural features of CTB and associated membranes in response to low pH. Fluorescence resonance energy transfer (FRET) was used to monitor the relative positions of Trp88 and extrinsic probes covalently linked to CTB, the hydrophobic tail of GM1, and the polar surface of GM1-containing PC vesicles. Acidic pH does not significantly influence the distance from Trp88 to extrinsic probes on (1) CTB, (2) the membrane-imbedded tail of GM1, or (3) the surface of GM1-containing membranes. In contrast, low pH does influence the position of other sites (Lys69 and/or Lys91) on CTB relative to a pyrene probe on the nonpolar acyl tail of GM1 and polar NBD probes located at the membrane surface. Moreover, while low pH does not promote release of CTB from pyrene-GM1 or extraction of pyrene-GM1 from membranes, it does cause the pyrene group on the nonpolar tail of GM1 to approach the membrane surface. These findings agree with previous suggestions that CTB association with GM1-containing membranes results in a localized disturbance of membrane phospholipid packing and that this phenomenon can be specifically influenced by acidic pH (*17*, *36*). Whether these events are related to the endosomal processing of CT is not yet known.

The fluorescence experiments described here provide evidence that low pH induces specific conformational changes in CTB that directly influence membrane structure at the site of CTB binding. The physiological significance of these data is supported by the fact that fluorescent derivatives of GM1 are capable of serving as CT receptors when incubated with cells lacking GM1 and are able to restore CT sensitivity to these cells (*56*). An interesting aspect of the data presented here is the possibility that the central α-helix of CTB may be participating in the observed pH-dependent conformational transitions of CTB. Lys69 appears to be one of two sites that readily label with extrinsic fluorescent probes under the labeling conditions used here. The fact that ligand binding results in an ordering of amino acids at the C-terminus of the A2 polypeptide of the closely related heat-labile enterotoxin of *E. coli* (*27*) suggests that receptor binding prompts the relay of structural signals to the central α-helices of the B subunit of this CT relative. It is likely that similar structural signals occur in CT even though the C-terminal residues of CTA2 are highly ordered even before GM1 is bound (*25*).

A possible complicating factor for the data presented here is uncertainty about the nature of the contributions that a second labeling site (Lys91) has on the observed results. The presence of Lys91 in a loop between *β*-strands 5 and 6 of CTB suggests that it is somewhat flexible in the absence of GM1; however, the terminal galactose residue on the pentasaccharide of GM1 has been shown to bind near Lys91, which probably would sterically limit the mobility of a probe at this position in the presence of ganglioside (*23*). Fortunately, low pH does not dramatically influence the position of Trp88 relative to the membrane surface (Figure 6) and has no effect on the distance from Trp88 to the probe on pyrene-GM1 (Figure 1). Because the extrinsic probe on Lys91 is close to Trp88, it is likely to behave in a similar manner and thus its influence would not overshadow the observed pH-dependent distance changes unless it was present in large excess over the probe at Lys69. It is likely, however, that the magnitude of the structural changes seen here is influenced by the presence of labeling at Lys91.

Because low pH results in an apparent movement of extrinsic probes on CTB (a large percentage of which are on the central α-helix of CTB) away from the membrane-imbedded tail of pyrene-GM1 but toward the membrane surface, this could indicate that the central pore of the CTB pentamer changes shape under low-pH conditions. Such a shape change could be explained by a model like that described in Figure 7. A label on the central α-helix of a single CTB monomer (Figure 7, top panel) (*57*) could approach the membrane surface while moving away from the hydrophobic tail of GM1 if the helix were to rotate relative to the plane of the membrane surface (Figure 7, middle and bottom panels). Concurrent distortion of the position occupied by GM1 within the membrane could contribute further to this observation and result in the hydrophobic tail of GM1 coming closer to the membrane surface. When the central α-helices on the entire CTB pentamer are then considered, the outcome could resemble the irislike movement suggested by London for the CTB pentamer (*58*). Such a change in shape could have a profound effect on the way CTB influences membrane packing (*36*) and on the ability of CTB to form anionic channels (*17*). Initial disruption of membrane packing by CTB has been proposed to be due to the rigid placement of five GM1 molecules within the membrane following association with CTB (*21*). This could create a geometry in which the area able to be occupied by phospholipids is reduced by 25% or more between the fixed positions of five GM1 molecules bound by the CTB pentamer (*21*). If this is the case, a pH-dependent modification of phospholipid packing could reflect a change in the position of one GM1 binding site on the CTB pentamer relative to another. Significant structural changes such as these could have a

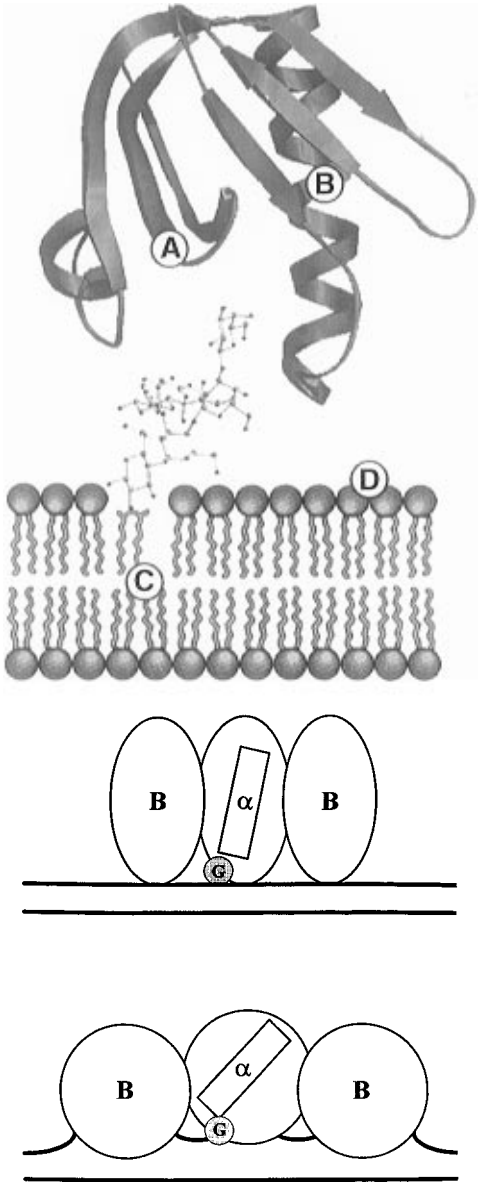

FIGURE 7: Movement of fluorescent probes within the CTB/membrane complex. In the top panel, the ribbon structure for a single CTB monomer is shown above a phospholipid bilayer from which the oligosaccharide moiety of GM1 protrudes. The relative positions of fluorescent probes are A, Trp88; B, CPI, FITC, or SITS at Lys69; C, pyrene-GM1; and D, NBD-PE or fluorescein-DHPE. Extrinsic labeling of CTB also occurred at Lys91 located on the loop near Trp88 (not shown). In the middle panel, the CTB monomer at neutral pH is depicted as an oval with the central α-helix represented by a rectangle that is nearly perpendicular to the plane of the membrane below. In the bottom panel, subtle conformational changes in the monomer may occur as the pH is lowered that alter the overall shape of the monomer and possibly cause the central α-helix to become more parallel with the membrane surface. This would bring a probe on Lys69 closer to the membrane as it moves away from the hydrophobic tail of GM1, which is displaced slightly from its original position within the membrane. Movement of the GM1 could result in its hydrophobic tail approaching the membrane surface without actually coming into contact with the aqueous phase, which would either place stress on or release stress from the packing of phospholipids beneath the CTB pentamer. The membrane structure in the bottom panel is shown as being distorted; however, it appears to be unlikely that CTB actually enters into the hydrophobic core of the membrane (*19*). The protein model shown in the top panel was made using the program Ribbons of Carson (*57*).

major impact on the endosomal processing, targeting, and adjuvanticity of CT following uptake by target cells.

ACKNOWLEDGMENT

We acknowledge assistance from Dr. Tom Hassell (Sigma Chemical Co.) for mass spectrometry, RP-HPLC, and peptide sequence analyses and Heather Felton for carefully reading the manuscript.

REFERENCES

1. Cassel, D., and Pfeuffer, T. (1978) *Proc. Natl. Acad. Sci. U.S.A. 75*, 2669−2673.
2. Finkelstein, R. A. (1988) in *Immunochemical and Molecular Genetic Analysis of Bacterial Pathogens* (Owens, P., and Foster, T. J., Eds.) pp 85−102, Elsevier, New York.
3. Spangler, B. D. (1992) *Microbiol. Rev. 56*, 622−647.
4. Sattler, J., Schwarzmann, G., Knack, I., Rohm, K.-H., and Wiegandt, H. (1978) *Hoppe-Seyler's Z. Physiol. Chem. 359*, 719−723.
5. Goins, B., and Freire, E. (1988) *Biochemistry 27*, 2046−2052.
6. Schön, A., and Freire, E. (1989) *Biochemistry 28*, 5019−5024.
7. Galloway, T. S., and van Heyningen, S. (1987) *Biochem. J. 244*, 225−230.
8. Moss, J., and Vaughan, M. (1988) *Adv. Enzymol. Relat. Areas Mol. Biol. 61*, 303−379.
9. Peterson, W. J., and Ochoa, L. G. (1989) *Science 245*, 857−859.
10. Harokopakis, E., Childers, N. K., Michalek, S. M., Zhang, S. S., and Tomasi, M. (1995) *J. Immunol. 185*, 31−42.
11. Holmgren, J., Lycke, N., and Czerkinsky, C. (1993) *Vaccine 11*, 1179−1184.
12. Mestecky, J. (1987) *J. Clin. Immunol. 7*, 265−272.
13. Dertzbuagh, M. T., and Elson, C. O. (1991) in *Topics in Vaccine Adjuvant Research* (Sprigg, D., and Koff, W., Eds.) pp 119−135, CRC Press, Boca Raton, FL.
14. Liang, X., Lamm, M. E., and Nedrud, J. (1988) *J. Immunol. 141*, 1495−1501.
15. Russell, M. W., and Wu, H.-Y. (1991) *Infect. Immun. 59*, 4061−4070.
16. Lycke, N., Karisson, U., Sjolander, A., and Magnusson, K. E. (1991) *Scand. J. Immunol. 33*, 691−698.
17. Krasilnikov, O. V., Muratkhodjaev, J. N., Voronov, A. E., and Yezepchuk, Y. V. (1991) *Biochim. Biophys. Acta 1067*, 166−170.
18. Tosteson, M. T., and Tosteson, D. C. (1978) *Nature (London) 275*, 142−144.
19. Wisnieski, B. J., and Bramhall, J. S. (1981) *Nature (London) 289*, 319−321.
20. Reed, R. A., Mattai, J., and Shipley, G. G. (1987) *Biochemistry 26*, 824−832.
21. Ribi, H. O., Ludwig, D. S., Mercer, K. L., Schoolnik, G. K., and Kornberg, R. D. (1988) *Science 239*, 1272−1276.
22. Zhang, R.-G., Westbrook, M. L., Westbrook, E. M., Scott, D. L., Otwinowski, Z., Maulik, P. R., Reed, R. A., and Shipley, G. G. (1995b) *J. Mol. Biol. 251*, 550−562.
23. Merritt, E. A., Sarfaty, S., van der Akker, F., L'Hoir, C., Martial, J. A., and Hol, W. G. J. (1994) *Protein Sci. 3*, 166−175.
24. Merritt, E. A., Sixma, T. K., Kalk, K. H., van Zanten, B. A. M., and Hol, W. G. J. (1994) *Mol. Microbiol. 13*, 745−753.
25. Zhang, R.-G., Scott, D. L., Westbrook, M. L., Nance, S., Spangler, B. D., Shipley, G. G., and Westbrook, E. M. (1995) *J. Mol. Biol. 251*, 563−573.
26. Sixma, T. K., Pronk, S. E., Kalk, E. H., Wartna, E. S., van Zanten, B. A. J., Witholt, B., and Hol, W. G. J. (1991) *Nature (London) 351*, 371−378.
27. Sixma, T. K., Pronk, S. E., Kalk, K. H., van Zanten, B. A. M., Berhuis, A. M., and Hol, W. J. G. (1992) *Nature 355*, 561−564.
28. Cabral-Lilly, D., Sosinsky, G. E., Reed, R. A., McDermott, M. R., and Shipley, G. G. (1994) *Biophys. J., 66*, 935−941.
29. Orlandi, P. A., and Fishman, P. H. (1993) *J. Biol. Chem. 268*, 17038−17044.
30. Houslay, M. D., and Elliott, K. R. F. (1981) *FEBS Lett. 128*, 289−292.

31. Janicot, M., Fouque, F., and Desbuquois, B. (1991) *J. Biol. Chem. 266*, 12858−12865.
32. Lencer, W. I., Delp, C., Neutra, M. R., and Madara, J. L. (1992) *J. Cell Biol. 117*, 1197−1209.
33. Lencer, W. I., Moe, S., Rufo, P. A., and Madara, J. L. (1995) *Proc. Natl. Acad. Sci. U.S.A. 92*, 10094−10098.
34. Nambiar, M. P., Oda, T., Chen, C., Kuwazuru, Y., and Wu, H. C. (1993) *J. Cell. Physiol. 154*, 222−228.
35. Orlandi, P. A., Curran, P. K., and Fishman, P. H. (1993) *J. Biol. Chem. 268*, 12010−12016.
36. Picking, W. L., Moon, H., Wu, H., and Picking, W. D. (1995) *Biochim. Biophys. Acta 1247*, 65−73.
37. Madshus, I. H., Wiedlocha, A., and Sandvig, K. (1994) *J. Biol. Chem. 269*, 4648−4652.
38. Saleh, M., and Gariepy, T. (1993) *Biochemistry 32*, 918−922.
39. Sonnino, S., Acquotti, D., Riboni, L., Giuliani, A., Kirschner, G., and Tettamanti, G. (1986) *Chem. Phys. Lipids 42*, 3−26.
40. Stern, D., and Volmer, M. (1919) *Phys. Z. 20*, 183−188.
41. Laemmli, U. K. (1970) *Nature (London) 227*, 680−685.
42. Lakowicz, J. R. (1983) *Principles of Fluorescence Spectroscopy*, Plenum Press, New York.
43. Haas, E., Katchalski-Katzir, E., and Steinberg, I. (1978) *Biochemistry 17*, 5064−5070.
44. Wu, P., and Brand, L. (1994) *Anal. Biochem. 218*, 1−13.
45. dos Remedios, C. G., and Moens, P. D. J. (1995) *J. Struct. Biol. 115*, 175−185.
46. Odom, O. W., Robbins, D. J., Lynch, J., Dottavio-Martin, D., Kramer, G., and Hardesty, B. (1980) *Biochemistry 19*, 5947−5954.
47. Förster, T. (1948) *Ann. Phys. (Leipzig) 2*, 55−75.
48. Dawson, W. R., and Windsor, M. W. (1968) *J. Phys. Chem. 72*, 3251−3260.
49. Highsmith, S., and Murphy, A. J. (1984) *J. Biol. Chem. 259*, 14651−14656.
50. De Wolf, M. J. S., Fridkin, M., and Kohn, L. D. (1981) *J. Biol. Chem. 256*, 5489−5496.
51. Kurosky, A., Markel, D. E., & Peterson, J. W. (1977) *J. Biol. Chem. 252*, 7257−7264.
52. Lai, C.-Y., Xia, Q.-C., and Salotra, P. T. (1977) *Biochem. Biophys. Res. Commun. 116*, 341−348.
53. De Wolf, M. S. J., Van Dessel, G. A. F., Lagrou, A. R., Hilderson, H. J. J., and Dierick, W. S. H. (1987) *Biochemistry 26*, 3799−3806.
54. Mertz, J. A., McCann, J. A., and Picking, W. D. (1996) *Biochem. Biophys. Res. Commun. 226*, 140−144.
55. Bhakuni, V., Xie, D., and Freire, E. (1991) *Biochemistry 30*, 5055−5060.
56. Spiegel, S. (1985) *Biochemistry 24*, 5947−5952.
57. Carson, M. (1991) *J. Appl. Crystallogr. 24*, 958−961.
58. London, E. (1991) *Mol. Microbiol. 6*, 3277−3282.

BI962996P